Cerebral Cortex, December 2020;30: 6296–6312

doi: 10.1093/cercor/bhaa186
Advance Access Publication Date: 20 July 2020
Original Article

ORIGINAL ARTICLE

Distributed Motor Control of Limb Movements in Rat Motor and Somatosensory Cortex: The Sensorimotor Amalgam Revisited

Andrew C. Halley[1], Mary K.L. Baldwin[1], Dylan F. Cooke[2], Mackenzie Englund[3] and Leah Krubitzer[1,3]

[1]Center for Neuroscience, University of California, Davis, CA 95618, USA, [2]Biomedical Physiology and Kinesiology, Simon Fraser University, Burnaby, BC V5A 1S6, Canada and [3]Department of Psychology, University of California, Davis, CA 95616, USA

Address correspondence to Leah Krubitzer, Krubitzer Laboratory, Center for Neuroscience, University of California, Davis, 1544 Newton Court, Davis, CA 95618, USA. Email: lakrubitzer@ucdavis.edu

Abstract

Which areas of the neocortex are involved in the control of movement, and how is motor cortex organized across species? Recent studies using long-train intracortical microstimulation demonstrate that in addition to M1, movements can be elicited from somatosensory regions in multiple species. In the rat, M1 hindlimb and forelimb movement representations have long been thought to overlap with somatosensory representations of the hindlimb and forelimb in S1, forming a partial sensorimotor amalgam. Here we use long-train intracortical microstimulation to characterize the movements elicited across frontal and parietal cortex. We found that movements of the hindlimb, forelimb, and face can be elicited from both M1 and histologically defined S1 and that representations of limb movement types are different in these two areas. Stimulation of S1 generates retraction of the contralateral forelimb, while stimulation of M1 evokes forelimb elevation movements that are often bilateral, including a rostral region of digit grasping. Hindlimb movement representations include distinct regions of hip flexion and hindlimb retraction evoked from S1 and hip extension evoked from M1. Our data indicate that both S1 and M1 are involved in the generation of movement types exhibited during natural behavior. We draw on these results to reconsider how sensorimotor cortex evolved.

Key words: sensorimotor, stimulation, motor, rat, evolution

Introduction

Which areas of the neocortex are involved in the generation of movements, and what are the common features of organization of these areas that are shared by all mammals? In most species, motor functions have traditionally been assigned to areas of the frontal lobe (e.g., primary motor cortex [M1]), though the number and organization of frontal motor areas differs across mammalian species. For example, primate motor regions include a primary motor area (M1), the supplementary motor area (SMA) and different divisions of premotor cortex (PMC). In rats, motor cortex has been divided into two cytoarchitectonic divisions. First, the medial agranular cortex (AGm) is involved in motor control of the vibrissae (e.g., Brecht et al. 2004). Second, the lateral agranular cortex (AGl) is involved in motor control of the postcranial body, including the forelimb, trunk, and hindlimb (e.g., Hall and Lindholm 1974). It remains unclear whether these regions compose a single cortical area, that is, M1 (Brecht et al. 2004) or two distinct cortical areas, that is, M1 and M2 (Donoghue and Wise 1982; Neafsey et al. 1986). Given that primary and secondary sensory cortical fields are often defined by complete

representations of the contralateral sensory epithelium (e.g., Kaas 1982), it may be parsimonious to define motor cortex using similar criteria and consider AGl and AGm to be a single cortical field (M1).

Early work using both short-train (ST-) intracortical microstimulation (ICMS) and electrophysiological recording led to the proposal that rats and other rodents exhibit a partial overlap of S1 and M1 body maps in the hindlimb and forelimb (Hall and Lindholm 1974). In fact, evidence for this partial "amalgam" of the somatosensory and motor maps in rats has played a central role in a major theory of motor cortex evolution in mammals (Lende 1969; see Discussion). Although sometimes overlooked, other studies have found evidence that movements can be evoked from portions of S1 "outside" the traditional "overlap" region, including barrel cortex in rats (Gioanni and Lamarche 1985; Neafsey et al. 1986) and mice (Matyas et al. 2010). Despite this compelling evidence that most of S1 is involved in motor control (cf., Woolsey 1958), the traditional view that M1 partially overlaps the hindlimb and forelimb representations of S1 forming an incomplete amalgam still persists (e.g., Frost et al. 2000).

In recent years, the technique of long-train (LT-) ICMS has been used to study complex movement types in diverse species. Though the use of longer stimulation durations has generated considerable debate (e.g., Strick 2002; see Discussion), it has revealed a number of features of motor organization that were obscured by traditional ST-ICMS methods. First, movements that are elicited with ST-ICMS are usually truncated versions of the more complex, multi-joint muscle synergies that are elicited from LT-ICMS (e.g., Graziano et al. 2002; Baldwin et al. 2017a). Second, classic studies describe the movements elicited with ST-ICMS at the most minimal conditions of stimulation (shortest duration and lowest current). Longer duration and higher current stimulation, which often elicits a suite of multi-joint movements or muscle synergies (Graziano et al. 2002), can reveal details of motor cortex organization that are not exhibited at threshold stimulation.

Interestingly, LT-ICMS has demonstrated that movements can be elicited from cortical areas that are located outside of traditionally defined motor regions in frontal cortex (e.g., M1, M2, SMA, and PMC), even at low currents. Recent LT-ICMS studies in a variety of mammals including tree shrews, prosimian galagos, capuchin monkeys, and macaque monkeys demonstrate that movements can be evoked by stimulation of somatosensory cortex (areas 3a, 3b, 1, 2) and posterior parietal cortex (PPC) (e.g., Cooke et al. 2003; Stepniewska et al. 2005; Gharbawie et al. 2011; Rathelot et al. 2017; Baldwin et al. 2017a; Baldwin et al. 2018; Mayer et al. 2019). This raises the possibility that in the rat, LT-ICMS could reveal motor functions in S1 beyond the sensorimotor "amalgam" described by traditional ST-ICMS techniques.

LT-ICMS studies in rats have focused on complex forelimb movements elicited from stimulation of two distinct forelimb representations in motor cortex. These regions are termed the caudal and rostral forelimb areas (CFA and RFA; Neafsey and Sievert 1982; Bonazzi et al. 2013; Brown and Teskey 2014; Deffeyes et al. 2015). Studies of connections of CFA and RFA indicate that they both send direct projections to the spinal cord, although each region has unique patterns of cortical and thalamic connections (Donoghue and Wise 1982; Neafsey and Sievert 1982; Rouiller et al. 1993). Unfortunately, CFA and RFA are usually defined relative to Bregma coordinates rather than the architectonically defined boundaries of M1 or S1, making it difficult to assign the location of stimulation sites to histologically defined cortical fields. It also remains unclear whether the complex movement types of other body parts (e.g., the hindlimb) are similarly distributed across motor areas.

The goal of the current investigation was to generate high-density maps of movement representations in both frontal and parietal cortex in rats using LT-ICMS to determine what kinds of movements are elicited, how these movement types relate to cortical fields defined histologically (e.g., M1 vs. S1), and how movements elicited with ST-ICMS and LT-ICMS techniques differ. In contrast to previous studies that have used LT-ICMS to characterize forelimb movements in rats (e.g., Ramanathan et al. 2006; Bonazzi et al. 2013; Brown and Teskey 2014), this investigation combined functional and histological analyses to describe how movement types are distributed across both S1 and M1 and examines a much greater extent of cortex (beyond CFA and RFA). By using identical ICMS parameters, histological techniques, and data analyses to those used in recent studies in other species, we can directly compare rat movement maps with those of tree shrews and primates (Cooke et al. 2003; Stepniewska et al. 2005; Gharbawie et al. 2011; Rathelot et al. 2017; Baldwin et al. 2017a; Baldwin et al. 2018; Mayer et al. 2019). This allows us to determine similar features of organization as well as those that are unique to different lineages and to make accurate inferences on the evolution of sensory and motor cortex in mammals.

Materials and Methods

Seven adult Sprague Dawley rats (2 males, 5 females; mean weight 265 ± 23 g; all adults, but exact ages are unknown) were used to characterize movements elicited in motor and somatosensory cortex using intracortical microstimulation (ICMS; see Table 1). In five of these cases, we produced high-density (mean = 92 sites) movement maps across most of the body representation using LT-ICMS in both frontal and parietal cortex. All experimental procedures were approved by UC Davis IACUC and conform to NIH guidelines.

Surgical Procedures

Animals were induced with a combination of isoflurane (2%), ketamine hydrochloride (70 mg/kg; IM), and xylazine (3 mg/kg; IM). Following initial induction, maintenance doses of ketamine (25%) and xylazine (25%) were given for the remainder of the experiment. Body temperature, respiration rate, eye-blink, and muscle tone were monitored throughout each experiment to assure steady levels of anesthesia.

Dexamethasone (1 mg/kg; IM) was administered to reduce brain swelling, and animals were placed into ear bars coated in 5% lidocaine cream. A subcutaneous injection of lidocaine (2%) was placed along the midline of the scalp, after which the skin and temporal muscles were retracted bilaterally to expose the skull. A large craniotomy was made spanning the entire frontal to midoccipital cortex of one hemisphere. The dura was retracted, and silicone fluid was applied to the cortical surface to prevent desiccation. Small screws were placed in the skull contralateral to the craniotomy (see below).

Animals were then transferred to a cloth hammock that allowed the forelimbs and hindlimbs to hang freely for the remainder of the experiment (see Baldwin et al. 2017a). A head post was attached to the screws in the skull using dental acrylic, and then secured to a stereotaxic frame.

Table 1 Details of cases included in this study

Case	Sex	Weight (g)	Figure	Stimulation duration (ms)	Movement sites/total sites tested
15-63[a]	M	226	Figure 4	500	72/101
15-65[a]	M	264	Figure 4	500	62/86
16-222[a]	F	282	—	500	40/74
16-227	F	275	—	500	29/65
17-114	F	295	Figure 5	500	81/113
17-196	F	250	Figure 5	500	58/85
17-219	F	263	Figure 6	50, 500	56/73

[a]Cases included both motor mapping and electrophysiological recordings.

ICMS Mapping

Electrical stimulation was delivered using a Grass S88 stimulator, two SIU6 stimulus isolation units, and tungsten microelectrodes (0.1–1.0 MΩ). To obtain high-density maps across a broad expanse of cortex, we used long-train stimulation (500 ms). In order to compare the differences of movement evoked with different durations of stimulation, in one case we used both short- (50 ms) and long-train (500 ms) stimulation at every site (see Table 1), alternating which train duration was applied first between sites. For each stimulation duration paradigm, biphasic pulses were delivered at 200 Hz, with a pulse phase of 0.2 ms, and the current ranged from 10 to 300 µA. An electrode was lowered perpendicular to the cortex using a micromanipulator to a depth of 1500–1600 µm. In a few laterally placed sites (~4%), the angle of the electrode was oblique to the cortical surface, and we stimulated at a depth of 1700–1800 µm. Electrode penetration sites were marked relative to surface vascular patterns on a printed, high-resolution digital image of the cortical surface (Fig. 1A).

Two observers confirmed each movement elicited by stimulation, and at many sites movements were video-recorded (Sanyo Xacti, 1920 × 1080 resolution, 60 f/s) against a scale bar and analyzed offline using frame-by-frame analysis of the displacement of body parts using the software Tracker (http://physlets.org/tracker/). For the duration of each stimulation train, a synchronized timing signal was sent to a speaker and an LED placed near the animal within the video frames. Movement thresholds were determined by lowering the amplitude to the minimal current from which movements could be elicited and either averaging that value with a subthreshold current (10 µA intervals from 1 to 150 µA; 50 µA intervals from 150 to 300 µA) or recording the current at which movements could be evoked 50% of the time. Maps shown in Figures 4–6 reflect suprathreshold movements. Similar procedures have been previously used in our laboratory (e.g., Cooke et al. 2012; Baldwin et al. 2017a, 2018).

LT-ICMS movements of the forelimb and hindlimb generally involve multiple joints and muscles (Fig. 2A–C). We categorized each evoked movement of the limbs in two ways and generated movement maps for each method. The first type of movement map illustrates the joints and body parts involved in each evoked movement (e.g., shoulder or elbow). The second type of movement map illustrates movement patterns that direct the limb in a given direction (e.g., forelimb retraction = upward toward the trunk, involving shoulder extension and elbow flexion; Fig. 2D–F).

Electrophysiological Recording

In two cases (15-63 and 15-65), coarse topographic maps were generated using multiunit electrophysiological recording techniques in somatosensory cortex. Recordings were made at each electrode site that was also stimulated using LT-ICMS. Microelectrodes were lowered to a depth of 600–800 µm perpendicular to the brain surface. Neural responses were amplified, filtered, and monitored through a speaker and on a computer screen. Cutaneous stimulation consisted of light taps, brushes across the skin, and deflection of hairs. Deep receptors were stimulated by hard taps, pressure, and limb manipulation. Details of somatosensory mapping and receptive field determination have been described previously by our laboratory (Seelke et al. 2012).

Histological Processing

Prior to perfusion, fiducial probes (fluorescent dyes) were placed at multiple cortical locations surrounding the ICMS-explored area to facilitate the alignment of functional data with histologically processed tissue. Animals were euthanized with an intraperitoneal injection of sodium pentobarbitol (>100 mg/kg), and were perfused transcardially with saline, followed by 2% paraformaldehyde, and then 2% paraformaldehyde with 10% sucrose. The brain was extracted, and each cortical hemisphere was separated from the basal ganglia, diencephalon, and brainstem. The cortex was then flattened under a glass slide, and postfixed in 4% paraformaldehyde for 0.5–2 h. Flattened cortex was then placed in 30% sucrose for 24–48 h prior to sectioning. The first 2–3 sections were cut at 60–80 µm and stained for cytochrome oxidase (CO) to reveal vascular patterns for functional alignment (see below; Fig. 1C). Following this, 30–40-µm sections were cut and processed for myelin and CO in alternating series. High-resolution scans of tissue were taken using a Nikon Multiphot (Tokyo, Japan) with a Phase One Powerphase FX1 scan back (Global Manufacturing, Louisville, CO). Scanned images were adjusted for brightness and contrast in Adobe Photoshop.

Alignment of Functional and Histological Data

In order to align functional maps directly to histologically/anatomically defined areal borders, photographs of the cortical surface used to document electrode sites in mapping experiments (Fig. 1A) were aligned with scans of myelin and CO stained tissue (Fig. 1C). First, each histological series was internally registered by aligning blood vessels across adjacent sections (Fig. 1B). Boundaries between cortical areas were

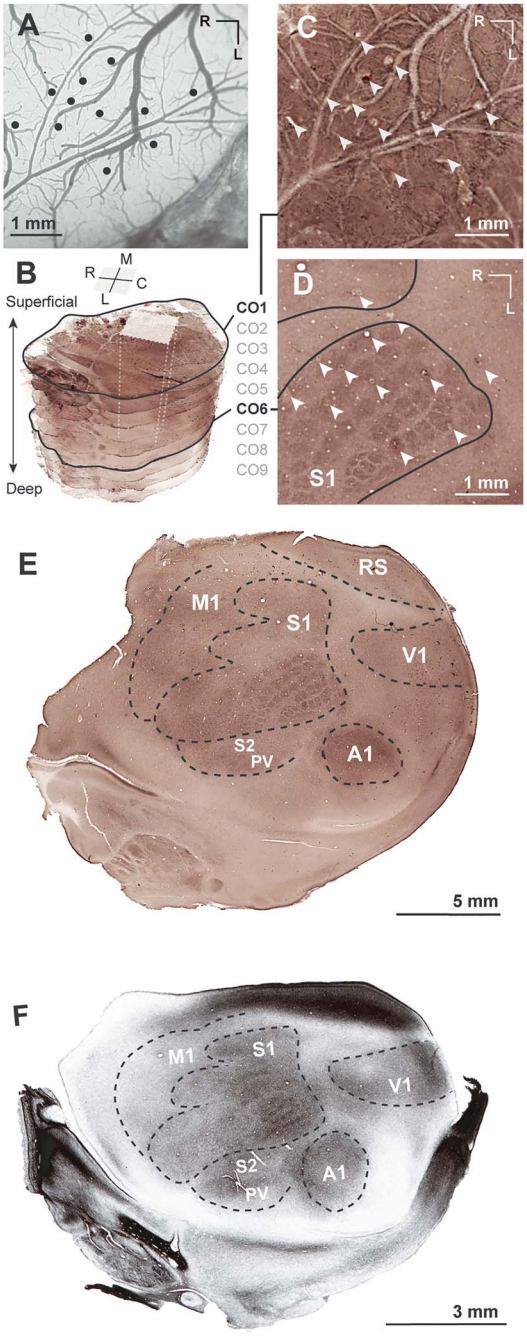

Figure 1. Methods for reconstruction of electrode sites from microstimulation experiments onto tangential sections of the rat cortex. (*A*) Photograph of the brain surface of case 15-65, with black dots indicating the location of electrode penetration sites where stimulation was applied. (*B*) Stacked image series of nine CO sections, with the most superficial (CO1) and layer 4 (CO6) sections outlined in black. The gray box and dotted lines within the image stack show the location of images of the two CO sections shown to the right. (*C*) The most superficial CO section shows surface vasculature and corresponds to the boxed region in *A*. Electrode penetrations are indicated by white arrows. (*D*) A deeper CO section, registered to the superficial section in *C* by aligning electrode tracts and vasculature, shows the whisker barrels in layer 4 of posterior medial barrel subfield (PMBSF). Electrode sites are indicated with white arrows. The borders of S1, including the PMBSF and the medially adjacent forelimb region, are indicated with black lines. (*E*) A whole left hemisphere stained for CO with borders drawn. (*F*) A whole left hemisphere stained for myelin with borders drawn. Whole brain sections in (*E*) and (*F*) are taken from different brains.

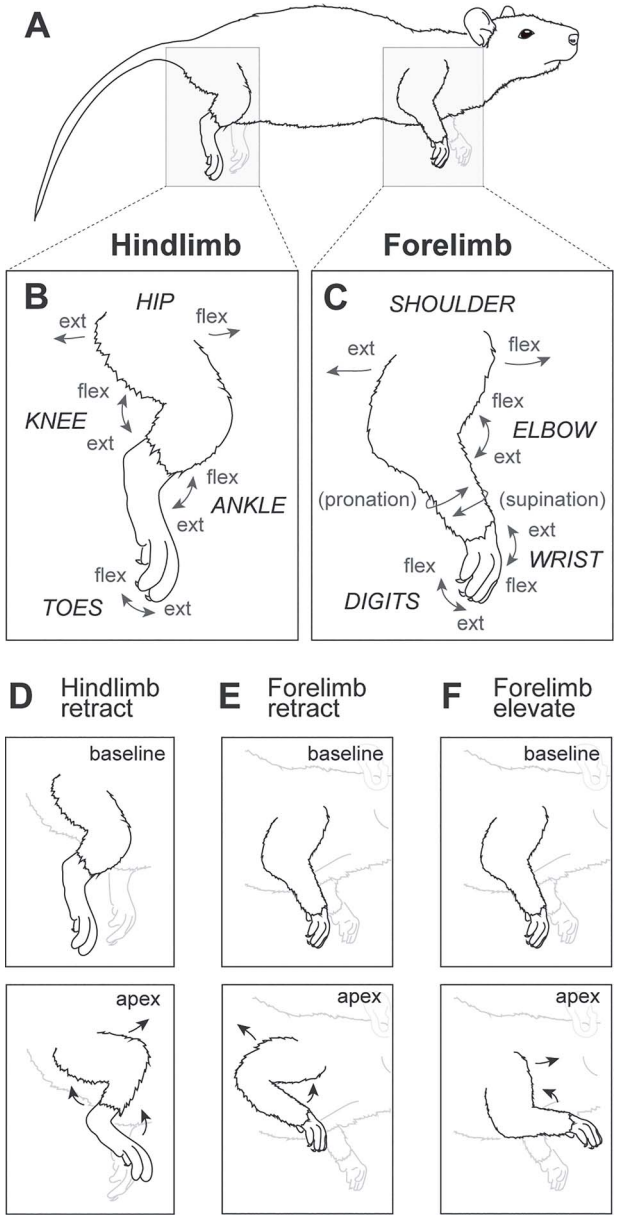

Figure 2. Types of forelimb and hindlimb movements in the rat. (*A*) A lateral view of the rat as it is positioned in a cloth hammock used in this study (see Methods and Materials). (*B*) Hindlimb movements include flexion and extension of the hip, knee, ankle, and toes. (*C*) Forelimb movements include flexion and extension of the shoulder, elbow, wrist, and digits, as well as pronation and supination of the forearm. (*D*) Hindlimb retraction involving hip flexion, knee flexion, and ankle flexion. (*E*) Forelimb retraction involving shoulder extension and elbow flexion. (*F*) Forelimb elevation involving shoulder flexion and elbow flexion. Drawings adapted from Liu et al. 2008.

delineated based on differential staining for myelin and CO across the series, and individual section borders were combined into a composite. Visible barrels in S1 (Fig. 1*D*) were outlined from CO sections. Electrode penetrations in processed tissue were identified relative to cortical surface vasculature as revealed by CO stains (Fig. 1*C*,*D*), as well as fiduciary probes. Functional maps were generated in Adobe Illustrator. Polygons surrounding electrode sites were generated using a Voronoi tessellation script for Adobe Illustrator (https://github.com/fabia

Table 2 Surface area (mm^2) of sites generating movements of individual body parts in five cases

	Case					Mean	SD
	15-65	15-63	17-114	17-196	17-219		
Total	61.45	42.36	56.02	29.14	39.65	45.72	13.00
Facial	46.90	28.35	41.39	19.27	22.88	31.76	11.92
Ears	11.15	4.48	—	—	—	7.82	4.71
Neck	2.97	0.96	—	—	—	1.97	1.42
Nose	—	0.53	7.79	0.53	—	2.95	4.19
Jaw	7.27	2.23	9.96	5.33	7.48	6.45	2.88
Vibrissae	30.31	22.34	29.27	14.01	17.90	22.77	7.06
CL (S1)	16.92	17.54	16.39	7.79	11.75	14.08	4.19
RM (M)	13.39	4.80	12.88	6.22	6.14	8.69	4.10
Forelimb	17.93	15.33	17.70	10.84	21.56	16.67	3.95
Shoulder	9.76	9.44	10.08	8.34	7.20	8.97	1.18
Elbow	12.54	10.79	15.48	7.09	17.84	12.75	4.16
Wrist	5.36	7.59	8.62	6.75	6.26	6.92	1.25
Digit	7.79	3.67	6.31	4.33	6.79	5.78	1.72
Trunk	1.36	7.46	3.69	5.28	3.42	4.24	2.27
Hindlimb	7.93	7.79	8.01	5.77	8.19	7.54	1.00

Totals are not simple sums of the constituent body parts, as many sites generated movements across the body.

nmoronzirfas/Illustrator-Javascript-Voronoi). Movement maps for each case were made by assigning each body part a color and tiling the polygon of each electrode site with colors for the body part movements evoked at that site. Maps of limb movement type for the forelimb and hindlimb were color-coded by assigning movement classes to each site (e.g., forelimb retraction vs. elevation). The location of bregma is noted on whole brain diagrams.

Quantification of Movement Types

In five cases with relatively complete movement maps, we measured the surface area (mm^2) of polygons generated from Voronoi tessellation in Adobe Photoshop, using the scale bar for each case (Table 2). We also calculated the percentage of each movement type as a proportion of the total surface area that elicited movements when stimulated (Table 3). Mean values and standard deviation (SD) were calculated for both surface area and percentage values, using only cases in which a particular movement type was observed at least once. Note that measurements include sites with multiple movement types, so body region measures do not add up to the total measures for either surface area or percentage. Measures are approximate, as the regions tested are not necessarily exhaustive (e.g., regions along the medial wall that were inaccessible in our experimental setup).

Composite Maps

To summarize the movements elicited across LT-ICMS cases and their relationship to histological borders, we aligned five cases from which we gathered high-density maps (73–113 sites per case) into a single composite map (methods shown in Fig. 3). Movement maps from individual cases were manually rotated and scaled to align histological landmarks that were easily identifiable in every case: 1) borders of S1; 2) the center of the S1 hindlimb region; 3) the caudal edge of the S1 forelimb region; 4) and the center of the S1 lower lip region. To include a more rostral landmark from the S1 region, the center of the representation in M1 from which jaw movements were evoked was included as an additional landmark (Fig. 3A,B). Once all five cases were aligned, the vector paths of S1 borders (Fig. 3B) were averaged using the Path Average tool in Adobe Illustrator, generating a single average S1 border for the composite map (Fig. 3C). A similar technique was used to produce an average landmark position for the four additional landmarks described above (Fig. 3C). Related methods have been used previously by our own and other laboratories to combine case data for connections (e.g., Hamadjida et al. 2016) and BOLD signal (e.g., Disbrow et al. 2000).

For each of the five high-density cases, Voronoi tiles from each site corresponding to a given movement (e.g., vibrissae; Fig. 3A) or limb movement type (e.g., forelimb retraction) were aggregated into a multi-tile polygon for that representation. Following alignment of the maps described above, these five polygons (one for each case) were superimposed (Fig. 3B). Finally, any area of overlap between 3 or more of the 5 cases was used to generate composite polygons (Fig. 3C), identifying regions of cortex where most cases exhibited that movement. For several movement types that were only observed in a few cases, a lower overlap threshold of 2/5 cases was permitted in composite maps, and this is labeled in Figure 7.

Results

Five experiments that resulted in high-density movement maps in both frontal and parietal areas of neocortex are described in detail and illustrated in Figures 4–6. The two additional experiments yielded similar results but are not presented as they had fewer sites or a smaller region of cortex was explored. We provide data on both the specific body parts from which movements were evoked (e.g., shoulder, hip) and the types of movements that were evoked (e.g., forelimb retraction vs. extension). In one case (17-219), we directly compare the forelimb and hindlimb movements elicited from both ST-ICMS and LT-ICMS at the same stimulation sites (Fig. 6; Supplementary Fig. 3). Finally, these five cases were averaged into composite maps (methods in Fig. 3), including both maps of body part movements, as well as limb

Table 3 Percentage of the surface area of excitable sites that generated movements of individual body parts in five cases

	Case (%)					Mean (%)	SD (%)
	15-65	15-63	17-114	17-196	17-219		
Total	100.0	100.0	100.0	100.0	100.0	100.0	—
Facial	76.3	66.9	73.9	66.1	57.7	68.2	7.3
Ears	18.1	10.6	—	—	—	14.4	5.3
Neck	4.8	2.3	—	—	—	3.6	1.8
Nose	—	1.3	13.9	1.8	—	5.7	7.1
Jaw	11.8	5.3	17.8	18.3	18.9	14.4	5.8
Vibrissae	49.3	52.7	52.2	48.1	45.1	49.5	3.1
CL (S1)	27.5	41.4	29.3	26.7	29.6	30.9	6.0
RM (M)	21.8	11.3	23.0	21.3	15.5	18.6	5.0
Forelimb	29.2	36.2	31.6	37.2	54.4	37.7	9.9
Shoulder	15.9	22.3	18.0	28.6	18.2	20.6	5.1
Elbow	20.4	25.5	27.6	24.3	45.0	28.6	9.6
Wrist	8.7	17.9	15.4	23.2	15.8	16.2	5.2
Digit	12.7	8.7	11.3	14.9	17.1	12.9	3.3
Trunk	2.2	17.6	6.6	18.1	8.6	10.6	7.0
Hindlimb	12.9	18.4	14.3	19.8	20.7	17.2	3.4

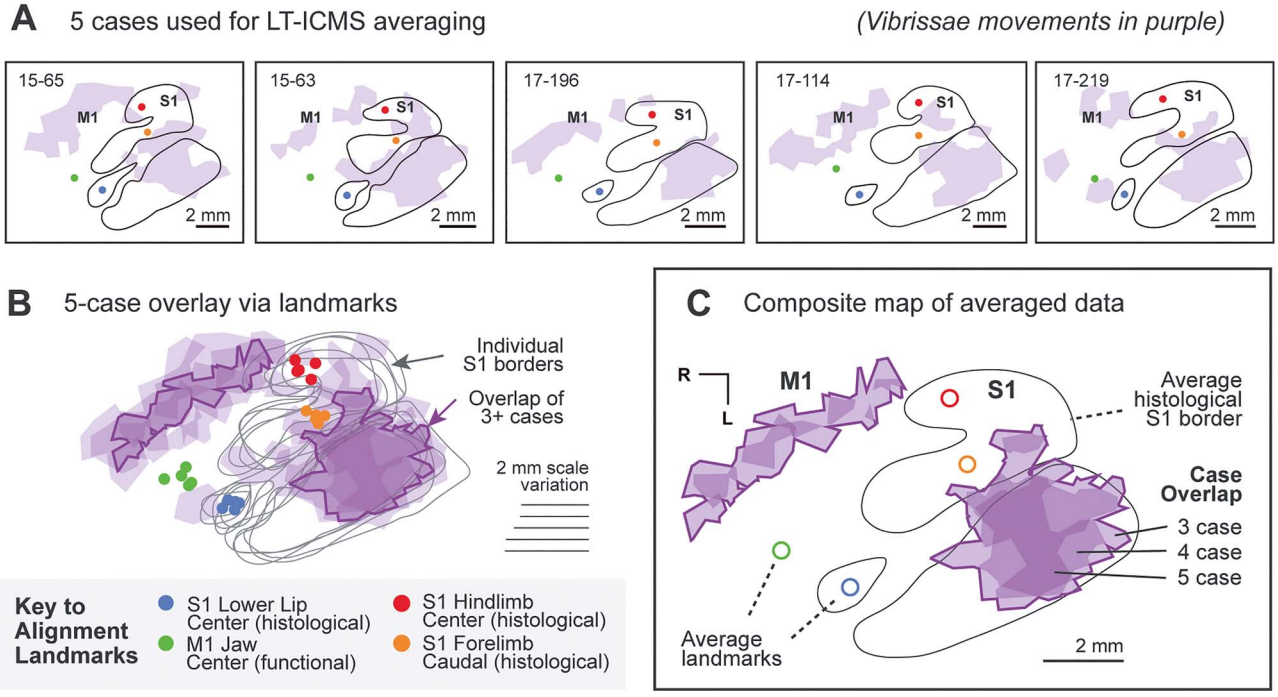

Figure 3. Methods for combining data across multiple cases to produce a composite map of movement types. (A) Five different cases with dense movement maps in M1 and S1 are included in our composite maps. Histologically defined borders of S1 are indicated by black lines, along with regions of neocortex from which movements of the vibrissae were evoked using LT-ICMS, shown in purple. Four landmarks on the cortex are indicated in each case: the center of the lower lip microvibrissae barrels of S1 (blue circle), the caudal edge of the forelimb region of S1 (orange circle), the center of the hindlimb region of S1 (red circle), and the functional center of the region of jaw opening in M1 (green circle). (B) All five cases are overlaid on top of one another and aligned (see Methods). Cases are rotated and scaled to minimize the distance between the histological borders of S1, as well as the four landmarks described above. Portions of M1 and S1 from which movements of the vibrissae were evoked are shown in purple. Gray lines indicate the borders of S1 for each of the five cases. The dark purple outlines surround regions where vibrissae representations were located in 3 or more cases. (C) A final composite map generated from 5 cases. The border of S1 (black line) is an averaged vector of the individual S1 borders shown in gray in B. The open shape landmarks indicate the average position of the landmarks for each of the five cases. Finally, the region in which 3 or more cases' vibrissae representation overlapped is shown in purple, with areas of minimal overlap having been removed from the previous step illustrated in B.

movement types (Fig. 7). Movement thresholds for two cases (15-63 and 15-65; Fig. 4) are shown alongside functional maps in Supplementary Figure 1. Somatosensory maps for these same two cases (15-63 and 15-65) are shown alongside LT-ICMS maps in Supplementary Figure 2.

Architectonic Determination of M1 and S1

We used a flattened cortex preparation to characterize cortical field borders with a high degree of accuracy, and to directly relate histological boundaries to functional results (Fig. 1). As

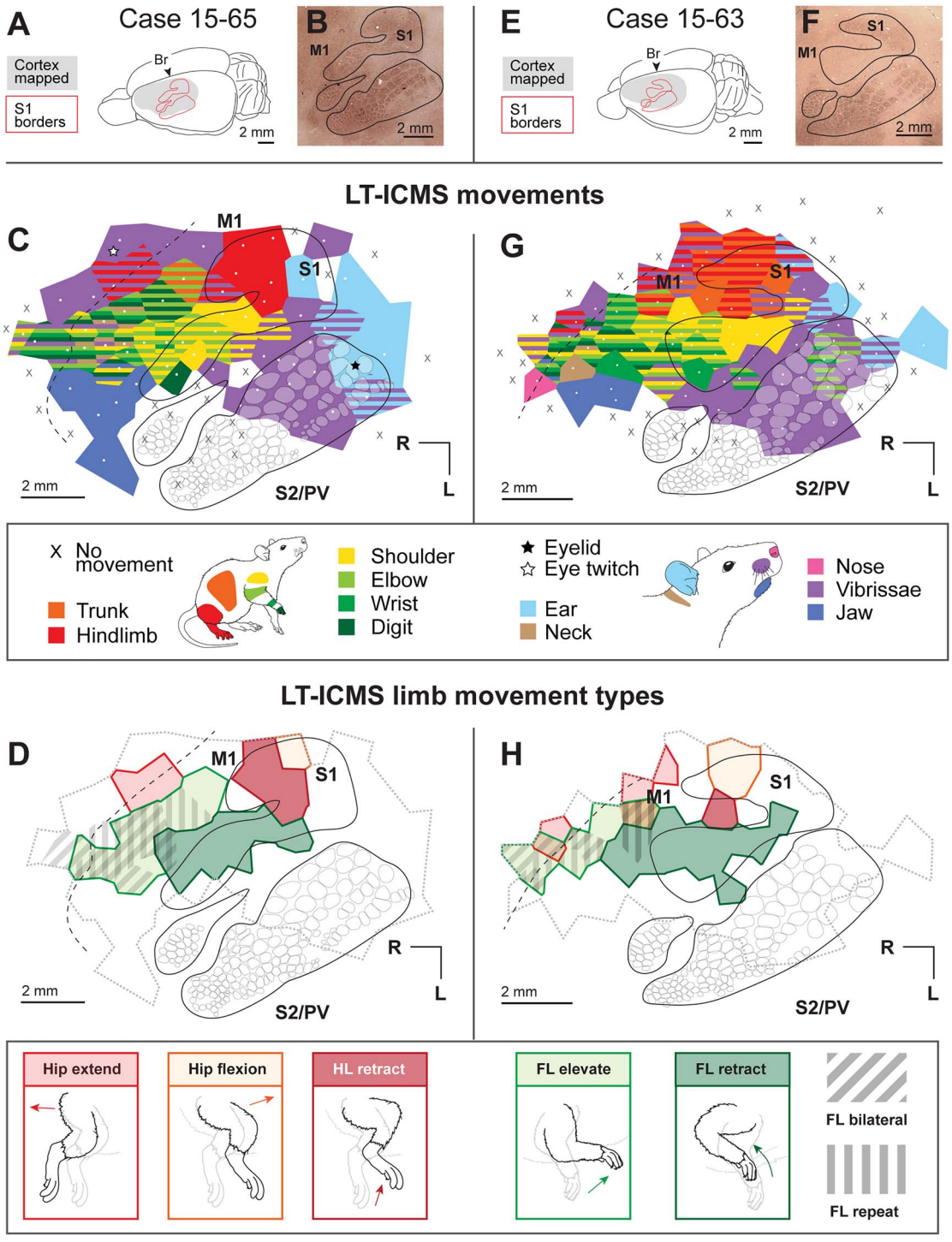

Figure 4. Movement maps produced from LT-ICMS in cases 15-65 and 15-63. (*A*) Dorsolateral view of the brain of case 15-65 indicating locations of S1 borders and the region that we explored using ICMS (gray). (*B*) A flattened section of cortex stained for CO, with S1 outlined. (*C*) Movement maps in S1 and M1 produced from LT-ICMS up to 300 µA. White dots indicate electrode penetration sites, with colored polygons indicating the body movements elicited from stimulation at that site. Black lines indicate the histologically determined border of S1. Opaque white round shapes indicate barrels identified from CO or myelin stains. The black dotted line indicates the approximate rostral border of M1 determined from myelin staining. (*D*) Forelimb and hindlimb movement types elicited from the same case. Evoked hindlimb movements include hip extension, hip flexion, and hindlimb retraction. Evoked forelimb movements include elevation in M1 and retraction in S1 and M1. Diagonal hatches indicate regions in M1 where bilateral forelimb movements were evoked, while vertical hatches indicate regions in M1 where repetitive forelimb movements were evoked. The grey dotted line indicates the area from which movements were evoked in (*C*). (*E–H*) Results from case 15-63, organized as in (*A–D*).

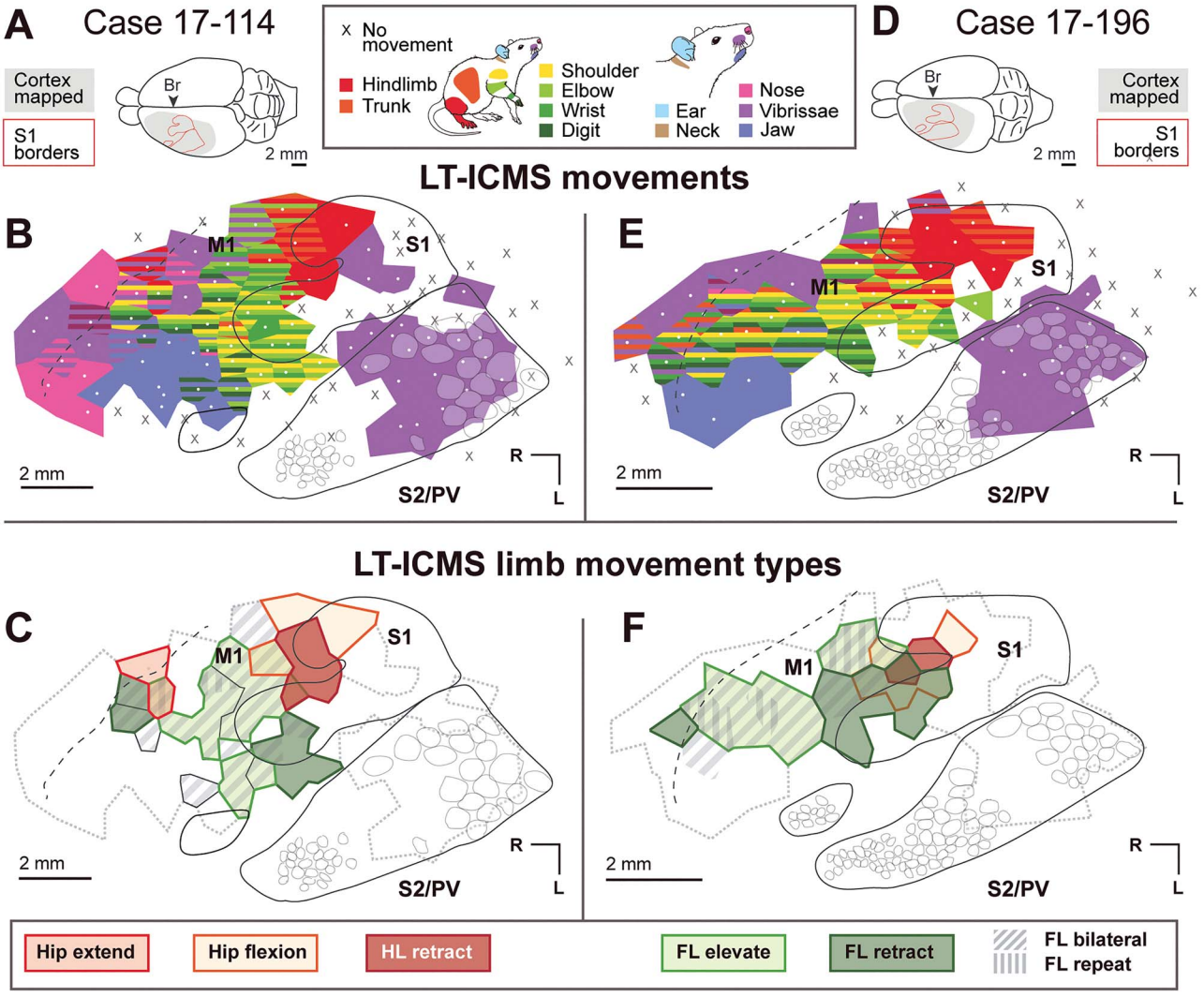

Figure 5. Movement maps produced from LT-ICMS in cases 17-114 and 17-196. (*A*) Dorsal view of the brain of case 17-114. (*B*) Movement maps in S1 and M1 produced from LT-ICMS up to 300 µA. White dots indicate electrode penetration sites, with colored polygons indicating the body movements elicited from stimulation at that site. Black lines indicate the histologically determined border of S1. Opaque white round shapes indicate barrels identified from CO or myelin stains. The black dotted line indicates the approximate rostral border of M1 determined from myelin staining. (*C*) Forelimb and hindlimb movement types elicited from the same case. The grey dotted line indicates the area from which movements were evoked in (*B*). (*D–F*) Results from case 17-196, organized as in (*A–C*).

described in previous studies in rats (e.g., Dawson and Killackey 1987; Remple et al. 2003) and other rodents (see Krubitzer et al. 2011), the primary somatosensory cortex (S1) has a distinct appearance in cortex that has been stained for CO (e.g., Fig. 4*B*,*F*) or myelin. In tissue stained for CO, S1 is heterogeneous in appearance and contains dark and light regions. The CO dense regions are coextensive with functionally defined cutaneous representations including the hindlimb, forelimb, trunk, face, and the well-established barrel field. These CO-dense regions are separated by CO light regions. The borders of the transitional zone (TZ) between S1 and M1, between the agranular medial (AGm) and agranular lateral (AGl) subregions of motor cortex, and at the rostral border of M1 were not distinct in our CO preparations. In sections stained for myelin, S1 is composed of myelin-dense regions separated with myelin-light regions. The myelin-dense regions are coextensive with CO-dense regions. M1 is more moderately myelinated than S1 and is bounded rostrally and laterally by lightly myelinated cortex. We define M1 as an architectonic subdivision coextensive with a movement map of the body and face and likely includes both AGl and AGm defined in previous studies. Using our techniques, it was not possible to define area 3a as distinct from M1 or 3b.

Organization of Movement Maps in M1 and S1

An important observation in the present investigation is that there are two cortical areas from which movements of most of the body could be evoked, S1 and M1. Rather than a partial overlap of the hindlimbs and forelimbs in S1 and M1 that is commonly reported as a partially overlapping amalgam (e.g., Hall and Lindholm 1974; Donoghue and Wise 1982; Tandon et al. 2008), we found a movement map of most of the body throughout the entire histologically defined S1, similar to one early report (Neafsey et al. 1986). Although movement maps

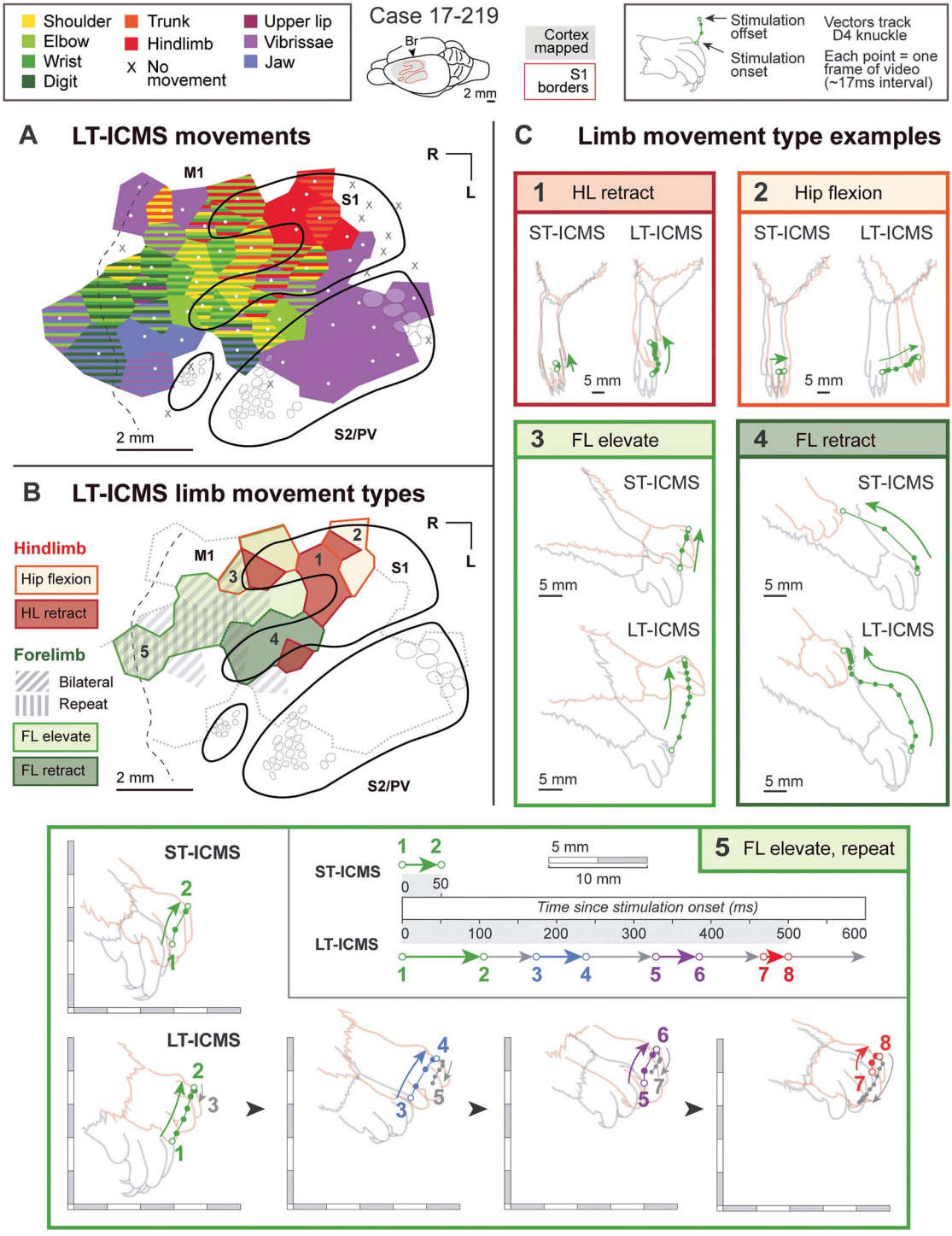

Figure 6. Movement maps produced from case 17-219, with a comparison of forelimb and hindlimb movements elicited with ST-ICMS (50 ms) and LT-ICMS (500 ms) at each site. As in Figures 4 and 5, the movement (*A*) and limb movement type (*B*) maps show the results of LT-ICMS in S1 and M1. (*C*) Movements elicited from both ST-ICMS and LT-ICMS at five sites indicated on the movement type map in (*B*). ST-ICMS generates small twitches which are frequently indistinguishable from one site to the next (e.g., compare ST-ICMS results at sites 3 and 5). Under LT-ICMS, movements evoked at these sites are different. Site 1 evoked a hindlimb retraction. Site 2 evoked a hip flexion, moving the hindlimb forward. Site 3 evoked a forelimb elevation. Site 4 evoked a forelimb retraction. Finally, Site 5 evoked a forelimb extension movement that was repetitive. LT-ICMS movements for Site 5 are broken into four segments to represent the repetitive nature of the movement.

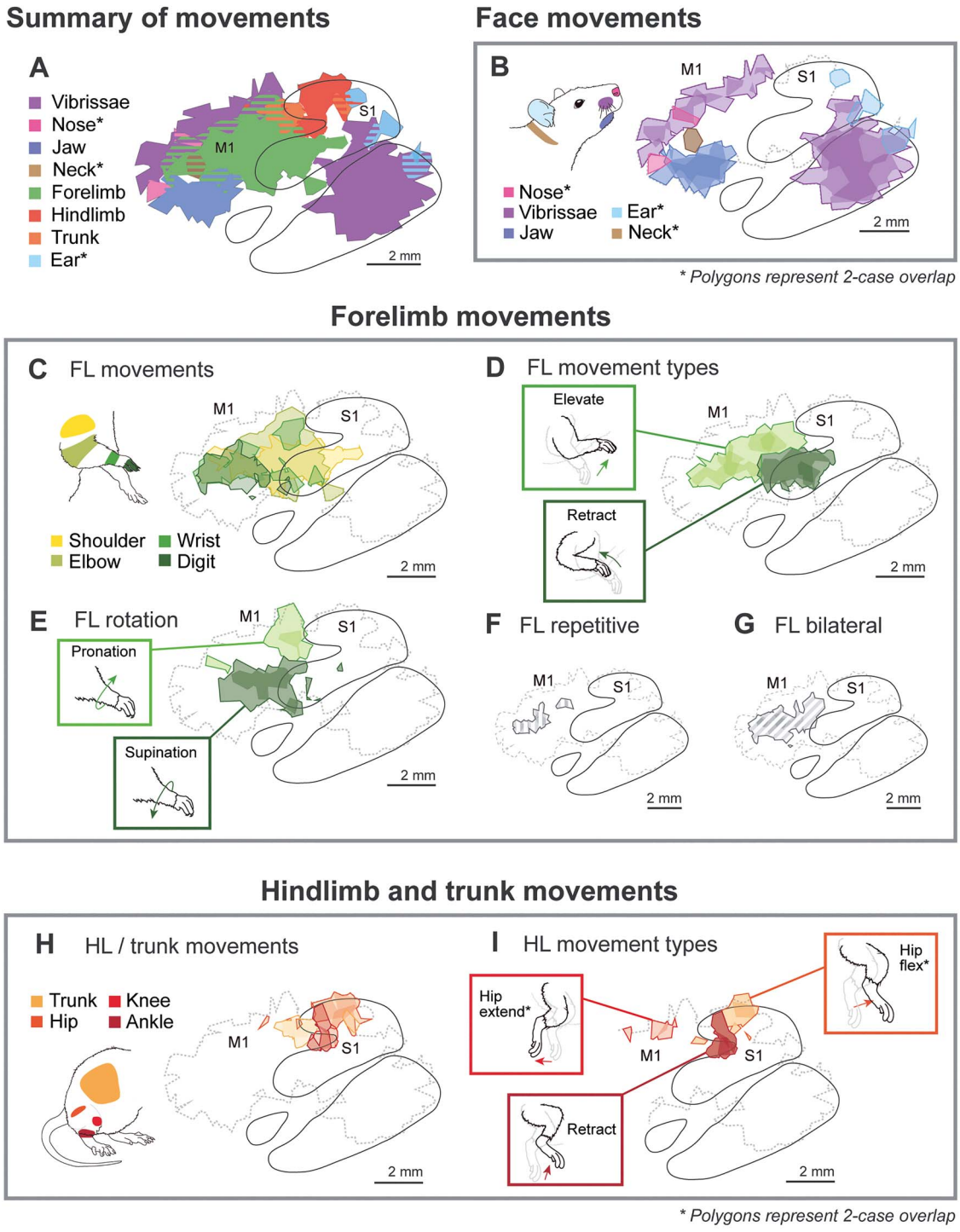

Figure 7. Composite maps generated from averaging the results of five high-density LT-ICMS maps. Methods are shown in Figure 3; the five cases included in the composite are shown in Figures 4–6. Polygons indicate the region of cortex from which a given movement type was evoked in 3 or more of the five cases, except where noted. The borders of S1 are an average vector of the S1 borders from the five individual cases (see Fig. 3B). (*A*) Summary of movements elicited for the hindlimb, forelimb, and face. Hatched regions indicate areas where more than one movement was elicited. (*B*) Facial movements were elicited from both S1 and M1. (*C*) Forelimb movements were evoked from a wide region of cortex ranging from the most rostral aspect of M1 to the middle of S1, with a concentration of digit movements in M1. (*D*) Stimulation sites which evoked forelimb retraction are concentrated in the S1 forelimb representation, while forearm elevation is evoked from a large portion of M1. (*E*) Forearm pronation and supination are evoked from distinct regions of M1. (*F*) Repetitive movements of the forelimb (see Fig. 6C, site 5) are evoked by LT-ICMS in the rostral portion of the M1 forelimb representation. (*G*) Bilateral forelimb movements are concentrated in M1. (*H*) Trunk and hindlimb movements are evoked from S1 and M1. (*I*) Hindlimb movements involving flexion of the hip, knee, and ankle (i.e., "retraction") are evoked from S1. Hip extensions are evoked from M1, while hip flexions are evoked from S1.

in M1 and S1 were fractured, there was a gross topographic representation of the body in each field, with the hindlimb represented medially followed by the forelimb and face more laterally (Fig. 7; see below).

Organization of Evoked Face and Head Movements from M1 and S1

Movements of the face were evoked from two separate regions of the neocortex, and are summarized in the composite map of Figure 7B. First, in the rostromedial portion of M1 we elicited movements of the vibrissae, nose, jaw, and neck. Here, vibrissae movements were elicited from a strip of neocortex bordering the medial wall, from the medial portion of S1 to the most rostral portions of M1 (Figs 4C,G and 5E). Movements of the nose were evoked from the rostral portion of M1 in three cases (Figs 4G and 5B,E). Movements of the neck were evoked in two cases (Fig. 4C,G) and were located within the forelimb representation, lateral to M1 vibrissae representations. Jaw movements were elicited in most cases in an area rostral to the S1 representation of the lower lip. Tongue movements evoked in other studies (e.g., Neafsey et al. 1986) were not evoked in this study, likely due to limited sampling rostral and lateral to the jaw representation of M1.

Quantification of movement types demonstrated that in every case, movements of the face (i.e., ears, neck, nose, jaw, and vibrissae) were elicited from more than half of the surface area of excitable cortex tested (mean = 68.2 ± 7.3%; Table 3). The movement representation of the face was dominated by the vibrissae, composing nearly half of the area of cortex from which movements could be evoked (mean = 49.5 ± 3.1%). Movements of the forelimb were also commonly evoked and occupied a relatively large region (mean = 37.7 ± 9.9%); these evoked movements most often included the shoulder and elbow. The average surface areas from which movement of the hip (10.6 ± 7.0%) and hindlimb (17.3 ± 3.4%) could be evoked were relatively smaller. Measurements for five cases are shown in Table 2 (surface area) and Table 3 (percentages). It should be noted that this quantification, while useful, is limited by the sampling density and the amount of cortex sampled in each case.

Movements of the vibrissae, ears, and eyelid were also evoked from the caudal and lateral portions of S1. Vibrissae movements in S1 were evoked in every animal studied ($n = 7$; see Figs 4–6), and largely overlapped with the posteromedial barrel subfield (PMBSF) as revealed in CO and myelin stains. In S1, ear movements were evoked in two cases (Fig. 4C,G), and eyelid movements were evoked in one case (Fig. 4C); each of these movement representations was located along the caudal boundary of the barrel field.

The only region of S1 from which movements were not elicited corresponds to the somatosensory representations of the tail located medially in S1, and the nose, buccal pad, lip and chin representations located in the rostrolateral portion of S1 (Remple et al. 2003; see Fig. 7B). However, evoked movements in many of these regions of S1 have been reported previously (Neafsey et al. 1986).

Organization of Evoked Forelimb Movements from M1 and S1

For each case, movements of the forelimb were analyzed according to major joints (i.e., shoulder, elbow, wrist, and digits), as well as according to limb movement types (i.e., retraction vs. extension, supination vs. pronation). Under our stimulation parameters (500 ms LT-ICMS), forelimb movements were elicited from a single, continuous region of cortex (summarized in Fig. 7C), rather than from distinct rostral and caudal regions separated by a representation of the neck (as previously reported in Neafsey and Sievert 1982; Tandon et al. 2008; Brown and Teskey 2014). In our single case in which both ST- and LT-ICMS was used, we found a continuous forelimb area with both stimulation paradigms (Supplementary Fig. 3B), even at lower thresholds (Supplementary Fig. 3C,D). In two cases, neck movements could also be evoked from this elongated forelimb representation (Fig. 4C,G), though in all but one of the stimulation sites in these cases, evoked neck movements were evoked in combination with movements of the forelimb. Further, the thresholds for evoked movements of the forelimb were equal to or below those of evoked movements of the neck in 5 of the 6 remaining sites. Stimulation sites that evoked digit flexion were also observed caudal to the neck representation in M1 in both cases.

Shoulder movements were evoked across most of the forelimb representation in both S1 and M1, with several cases having stimulation sites in which shoulder movements alone were elicited in the S1 forelimb representation (Fig. 4C,G). Evoked shoulder movements from S1 were mostly extensions (i.e., backward motion; Fig. 2C) as part of multi-joint forelimb retractions, while rostral shoulder sites in M1 usually evoked flexion (i.e., forward motion; Fig. 2C). Evoked movements of the elbow were similarly widespread in both S1 and M1, and primarily involved flexion. Wrist movements were evoked within the forelimb representation in S1 and at two locations within the forelimb representation of M1: the area immediately rostral to the S1 hindlimb representation, and the rostral-most region of M1 (Fig. 7C). Wrist movements included flexion, or flexion and extension in combination (see repeat movements below). Finally, evoked digit movements were observed in both S1 and M1 in most cases, although sites at which digit movements were evoked were concentrated in the rostral and lateral regions of the forelimb representation of M1 (Fig. 7C). Digit movements were usually observed in combination with wrist, elbow, and shoulder movements. Similar to the wrist representation, most stimulation sites in M1 evoked either digit flexion, or flexion and extension in combination (see repeat movements below).

In all cases, forelimb movements involving multiple joints were elicited from both S1 and M1, but the types of movements evoked were distinct from each other. First, LT-ICMS elicited retraction movements in the S1 forelimb representation that were generally characterized by shoulder extension and elbow flexion, drawing the entire forelimb backwards and upwards toward the trunk (Fig. 6C, site 4; Fig. 7D). By contrast, forelimb elevation movements were evoked from M1 and were characterized by shoulder flexion and elbow extension, moving the forelimb forward and then up (Fig. 6C, sites 3 and 5; Fig. 7D). Wrist and digit flexion were evoked from both the S1 and M1 forelimb representations, with a large region in which digit flexions could be evoked from the most rostral and lateral portions of M1 (Fig. 7C). In three cases we found sites in the medial portion of M1 in which we evoked pronation of the forearm, and lateral sites in which we evoked supination of the forelimb (Fig. 7E). Pronation of the forelimb was only evoked from the M1 forelimb representation, while supination of the forelimb was evoked from both the M1 and S1 forelimb representations (Fig. 7E).

Bilateral movements of the forelimb were evoked from M1 in most cases (Fig. 7G), and in the most rostral portions of

the S1 forelimb representation in some cases (Figs 5C and 6B). Evoked contralateral movements were always stronger than ipsilateral movements and generally involved the same forelimb muscle groups but were often opposite in the direction of movement (e.g., backward ipsilateral movement coupled with forward contralateral movement). Finally, repetitive movements of the forelimb were evoked under LT-ICMS (e.g., Fig. 6C site 5; Fig. 7F) at sites concentrated in the forelimb representation of M1, overlapping with the representation of digit flexion.

Organization of Evoked Trunk and Hindlimb Movements from M1 and S1

Trunk movements were primarily elicited from the region of M1 immediately rostral to the representation of the hindlimb in S1, and were observed in every case (Figs 4C,G, 5B,E and 6A). In three cases (Figs 4G, 5E and 6A) we also elicited trunk movements in S1, conjointly with movement of the hindlimb in the histologically defined hindlimb region.

Hindlimb movements were analyzed according to the major joints involved, and included movements of the hip, knee, and ankle. In every case, hip flexion, in which the entire hindlimb moved forward, was evoked from the S1 hindlimb representation (Fig. 7H,I). Immediately rostral to this hip representation, we found a representation in S1 in which knee and ankle flexions could be evoked (Fig. 7H); generating a retraction of the hindlimb upwards toward the body (Fig. 7I). Finally, in three cases (Figs 4C,G and 5B) we observed a separate representation of hip movements in M1. At these stimulation sites we evoked an extension of the hip in which the entire hindlimb moved backward (Fig. 7H,I).

Limb Movements Evoked using Short versus Long-train ICMS

In one case (Fig. 6) we compared the movements elicited at every site using both long (500 ms; LT-ICMS) and short (50 ms; ST-ICMS) durations of stimulation. The primary difference between ST-ICMS and LT-ICMS maps concerned the nature and duration of the movements elicited. In both the hindlimb (Fig. 6C, sites 1 and 2) and forelimb representations (Fig. 6C, sites 3–5) in M1 and S1, ST-ICMS generated movements that were truncated versions of those generated by LT-ICMS. The 50-ms duration of ST-ICMS movements is virtually identical to the first 50 ms of the movements generated under 500-ms LT-ICMS (Fig. 6C). Importantly, this means that some movements elicited from different sites that appear identical under ST-ICMS are revealed to be distinct under LT-ICMS. For example, two sites within the forelimb representation of M1 evoked similar slight elevation movements using ST-ICMS, but distinct movements using LT-ICMS. At one site (Fig. 6C, site 5) LT-ICMS evoked a complex repetitive movement. In the second site (Fig. 6C, site 3), LT-ICMS evoked an extended elevation that simply continued the ST-ICMS movement in the same direction (and without repetition). Finally, in this case, LT-ICMS thresholds are lower on average (96 μA; SD = 67 μA) than ST-ICMS thresholds (107 μA; SD = 79 μA; paired t-test; $t(51) = -3.11$; $P = 0.003$). These average measures reflect every site tested across the cortex (including S1 sites) and are therefore higher than traditional M1 thresholds reported in the rat.

Stimulation of Parietal Cortex Caudal to S1 (PM/PPC)

Stimulation of sites directly caudal to histologically defined S1 (i.e., the parietal medial area, PM, or PPC) generally failed to evoke movements in our experiments. In the few cases in which movements could be evoked from this region (Figs 4C,G and 5E), the stimulation sites were close to the caudal border of S1, and we evoked movements of either the vibrissae or nose.

Discussion

The current study in rats is one of a series of comparative studies in our laboratory designed to understand how neocortical networks involved in motor control have evolved. Specifically, we are interested in the frontoparietal networks associated with species-unique complex movement types (i.e., muscle synergies), and how these networks have been expanded and elaborated in different lineages, including primates. Here we discuss some of the pertinent previous studies of rat motor cortex and how they compare with the current investigation. We then compare the organization of motor cortex in other rodents and other mammals to infer which features of cortical organization are similar across clades, and which features have undergone changes in different lineages. In this section we also discuss issues associated with how to define cortical fields involved in motor control. Finally, we revisit the issue of the sensorimotor "amalgam" theory of mammalian evolution and propose revisions that incorporate more recent studies in rodents and other mammals.

Motor Cortex in Rats and Other Rodents

Like all eutherian mammals, rats and other rodents have both a primary somatosensory cortex (S1) and primary motor cortex (M1). Early studies on the organization of S1 and M1 in rats found that the topographic organization of cutaneous receptors of the body in S1 was an approximate mirror reversal of the movement maps in M1, with a region of partial overlap between the two fields (e.g., Hall and Lindholm 1974). Specifically, movements could be elicited from stimulation of two regions of S1: the most rostral portion of the forelimb representation, and the majority of the hindlimb representation. This partial sensorimotor "amalgam" in rats has played a central role in theories of cortical evolution (Fig. 8; discussed below). However, the ability to elicit movements is contingent on the stimulation parameters used (e.g., Neafsey et al. 1986) as well as anesthetic state (Sapienza et al. 1981; Tandon et al. 2008). In agreement with previous reports (e.g., Gioanni and Lamarche 1985; Neafsey et al. 1986) the current study demonstrates that movements can be elicited from stimulation of the majority of S1 in rats, including areas outside of the traditional sensorimotor overlap regions. For example, whisker movements can be elicited in barrel cortex even when stimulation is low amplitude and short duration (Supplementary Fig. 3; see also Gioanni and Lamarche 1985). The primary reason that some earlier studies failed to produce movements of the face in S1 (e.g., Hall and Lindholm 1974) is that this area was never explored.

Studies of motor cortex organization in other rodents are limited to mice and squirrels, and dense maps have only been determined for these species in a few studies (mice: Tennant et al. 2010; squirrels: Cooke et al. 2012). Using ST-ICMS these studies demonstrate that M1 contains a fractured topographic map, similar in organization to that described in the current

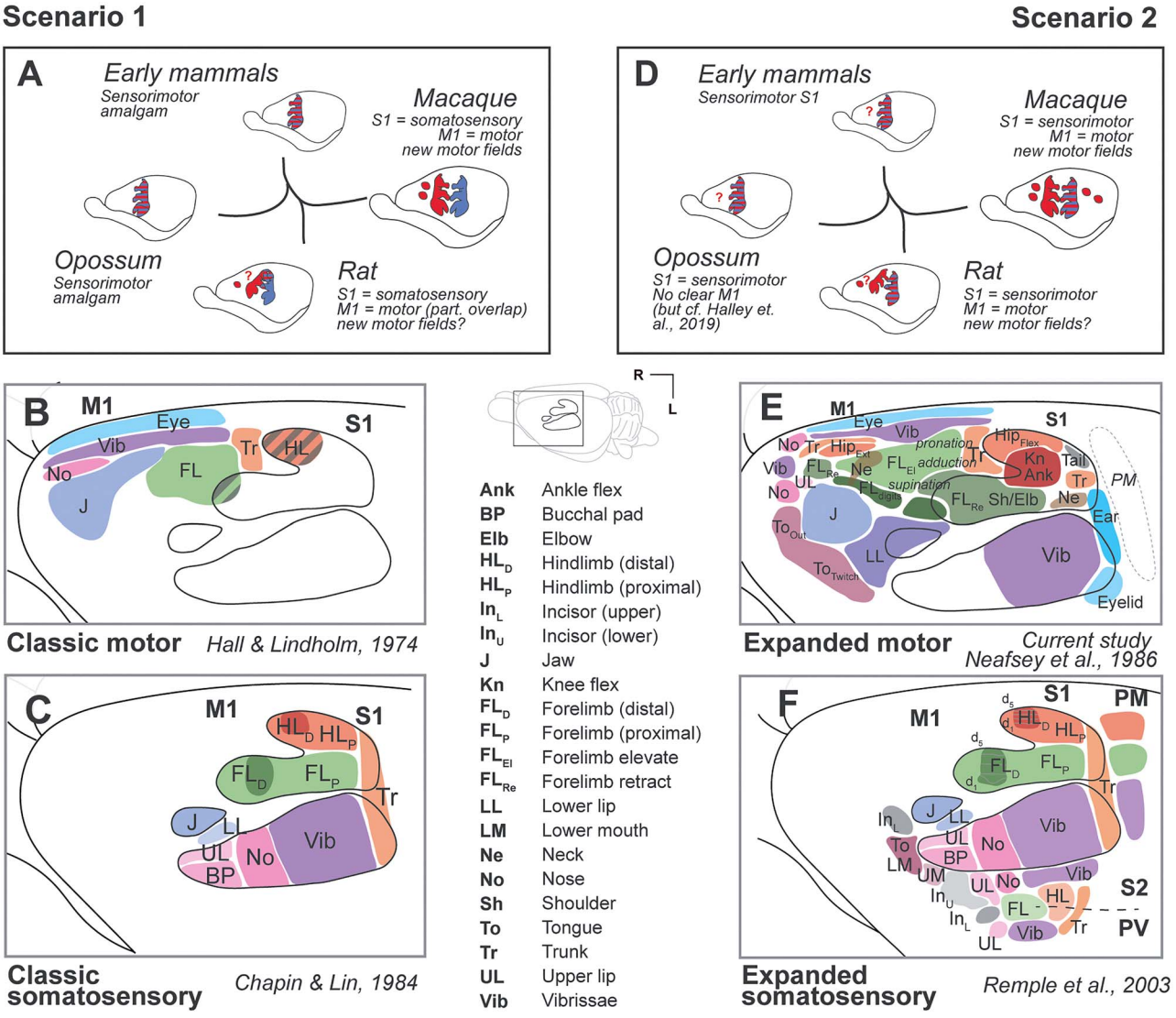

Figure 8. A number of theories have been proposed to explain the organization of sensory and motor areas in the neocortex of living mammals. The top of this figure shows two different theories of sensorimotor evolution in a highly simplified form, setting aside differences in cortical morphology between species in order to emphasize each theory's predictions. (*A*) Lende (1969) suggested that early mammals exhibited a sensorimotor "amalgam," meaning a single field with motor and sensory functions, and an overlapping topographic organization. While marsupials retained this ancestral "amalgam," eutherian mammals were proposed to exhibit a progressive segregation of motor and somatosensory functions. In rats, early studies on motor (*B*) and somatosensory (*C*) areas suggested that there was only a small region of sensorimotor overlap between the two fields (hatched section in *B*). This partial sensorimotor overlap in rats was proposed to represent an evolutionary step from an early mammalian amalgam (shared by living marsupials) and a higher-order segregation of sensory and motor functions, as observed in primates. (*D*) An alternative hypothesis argues that the earliest mammals had a cortical field similar to S1 in living species, with both sensory and motor functions, and that new motor fields (e.g., M1 and others) have been added in eutherian evolution. (*E*) Our study and others show that movements can be elicited throughout S1, and that these movement types are distinct from those elicited from stimulation of M1. (*F*) Somatosensory fields are also more diverse than originally thought, with multiple representations across the cortex with distinct functional attributes.

and previous studies in rats. In mice, a caudal forelimb representation was found in granular cortex (S1), although as in rats, it was considered to be a part of the M1 representation which overlapped with S1, rather than part of a separate movement representation within S1 (Tennant et al. 2010). Beyond forelimb movement areas, other studies in mice identified two spatially distinct locations, in M1 and S1, from which movements of the whiskers could be evoked (Matyas et al. 2010; Sreenivasan et al. 2015; Auffret et al. 2018), and a recent study found that orofacial movements associated with food consumption can be evoked from S1 (Clemens et al. 2018). In squirrels, only M1 and 3a were explored using ST-ICMS; S1 was not examined (Cooke et al. 2012). These studies indicate that, as in rats, motor control is not restricted to M1.

The current study expands on earlier work in several important ways. First, in our analysis, we describe all suprathreshold movements (rather than only the movements observed at threshold), which can reveal movement synergies between body parts. For example, we found combined movements of distinct body parts such as forelimb + hindlimb, forelimb + vibrissae, and vibrissae + ear. Second, evoked movements of different body parts are not strictly localized to their histologically identified,

isomorphic representations in S1, indicating that the overall movement representation of the body in S1 is not as precisely topographic as the sensory representation. For example, movements of the vibrissae could be evoked medially in conjunction with movements of the hindlimb in the CO identified hindlimb region, and movements of the hindlimb could be evoked in conjunction with the forelimb in CO identified forelimb region. Third, we demonstrate that bilateral movements can be evoked from M1 and S1, often from sites that represent multiple body parts, and that ipsilateral movements were often in the opposite direction of contralateral movements. Interestingly, a recent study in mice demonstrates a similar phenomenon in S1, where optogenetic stimulation produced contralateral whisker retraction and ipsilateral whisker protraction (Auffret et al. 2018), suggesting that the bilateral movement synergies, regardless of the body part, share common features (cf. Karadimas et al. 2020). The source of these evoked bilateral limb movements is not completely clear; however LT-ICMS (and ST-ICMS) is likely stimulating not just corticospinal neurons but is also activating local intrinsic circuits and perhaps even larger circuits, some of which may include contralateral representations. Finally, we show that the complex forelimb and hindlimb movements evoked from S1 are qualitatively different from those observed in M1. For example, forelimb movements evoked from S1 involve shoulder extension (backward movement) and elbow flexion, while those evoked from M1 involve shoulder flexion (forward movement), elbow extension, and wrist/digit flexion. It is possible that the retraction movements elicited in S1 are associated with sensitivity to touch and contribute to avoidance behaviors, and elevation movements in M1 may be associated with reach, object manipulation and exploratory behaviors.

Previous studies in rats also describe two separate forelimb movement representations in the neocortex, and these representations have been termed the rostral and caudal forelimb areas (RFA and CFA, respectively) (e.g., Neafsey and Sievert 1982; Bonazzi et al. 2013; Brown and Teskey 2014). While these two regions have been studied extensively, there is little consensus on what cortical areas the functionally defined RFA and CFA correspond to across studies in rats and across mammals. For example, some investigators consider RFA and CFA to be parts of M1 (e.g., Karl et al. 2008; Brown and Teskey 2014); while other investigators consider CFA to correspond to M1 and RFA to correspond to PMC in primates (e.g., Rouiller et al. 1993) or to the SMA of primates (e.g., Mohammed and Jain 2016). What is clear is that these functionally defined forelimb representations subserve different behaviors. For example, Brown and Teskey (2014) used reversible deactivation to show that RFA is associated with grasping and CFA is associated with reaching. Since RFA and CFA are generally defined using bregma coordinates, it is difficult to directly relate them to the current study, or to studies in other mammals. Nevertheless, the current study found that the retraction domain is largely contained within the forelimb region of S1. Finally, we found evidence in a few cases for a rostral hindlimb region in M1 (Figs 4C,G and 5B), and others have found evidence that a distinct area of M1 projects to the lumbar enlargement (Li et al. 1990).

Studies in mice also indicate a different role for S1 and M1 in motor control (Matyas et al. 2010). M1 controls rhythmic whisker protraction, while S1 controls short latency retraction. Sreenivasan et al. (2015) describe two parallel pathways that generate these distinct movement types across areas: first, an M1-brainstem pathway involved in rhythmic whisker protraction, and second, an S1-brainstem pathway involved in whisker retraction. Our data extends this previous work by demonstrating that movement types of the forelimb are similarly distributed across S1 and M1 and may be associated with different categories of exploratory versus avoidance behavior.

Motor Cortex in Other Mammals

Rodents are not the only mammals in which S1 plays a role in motor control, as demonstrated by comparisons with other mammals in which similar stimulation paradigms, histological preparations and data analysis techniques were used (Fig. 9). These studies demonstrate that movements can be elicited from both M1 and anterior parietal cortex (e.g., S1) in tree shrews (Baldwin et al. 2017a), bats (Halley et al. 2018), macaque monkeys (Gharbawie et al. 2011; Rathelot et al. 2017; Baldwin et al. 2018), capuchin monkeys (Mayer et al. 2019), marmosets (Burish et al. 2008), titi monkeys (Baldwin et al. 2017b) and galagos (Wu et al. 2000; Cooke et al. 2015). Early studies utilizing different stimulation paradigms also demonstrated that movements can be elicited from both S1 and M1 in squirrel monkeys (Welker et al. 1957) and even humans (Woolsey et al. 1979).

While S1 plays a role in generating movement in most species studied, important differences exist between species in the types of movements generated, and these differences are apparent across M1, S1, and other fields involved in motor control. From a comparative perspective, movement representations are strongly linked to body morphology, commonly used muscle synergies, and functional map organization. For example, primates with opposable thumbs have a large amount of cortical territory devoted to generating precise control of the digits including the thumb (Baldwin et al. 2018; Mayer et al. 2019); bats have a large cortical territory devoted to representing body parts involved in self-propelled flight (e.g., shoulder and hindlimb) as well as tongue-click echolocation (Halley et al. 2018), and rats have a large cortical territory devoted to the vibrissae and forelimb representations (Tables 2 and 3, current study). Compared with primates, a much smaller portion of M1 in rats has movement representations of the digits (Fig. 7C), and there appears to be no representation of digit movement alone.

Like other cortical fields (Kaas, 1983), motor areas of the neocortex are defined by a combination of their functional organization, cytoarchitecture, and connections with other brain areas. The fact that movements can be elicited from a variety of parietal regions in diverse species—far outside of traditionally defined motor cortical areas—requires that we revisit a basic question in neuroscience: which areas of the neocortex are involved in motor control? Given that extant mammalian species that are used as animal models have been independently evolving for 30–70 million years, the most accurate answer to this question must come from comparative research using multiple criteria for subdividing the neocortex.

One method for disentangling the extent to which M1 is necessary for activating circuits that ultimately elicit movement is the use of reversible deactivation to transiently inactivate areas of the neocortex, while stimulating others. This work has also informed a central methodological debate in motor research on the degree to which LT-ICMS causes “current spread” outside of the region of interest, either in proximity to the electrode, or in cortical regions connected to the stimulation site (e.g., Strick 2002). In both prosimian and New World primates, deactivation of M1 largely abolishes movements elicited from stimulation of posterior parietal cortex (PPC) (Cooke et al. 2015; Baldwin et al. 2017b). However, when M1 is deactivated in titi monkeys,

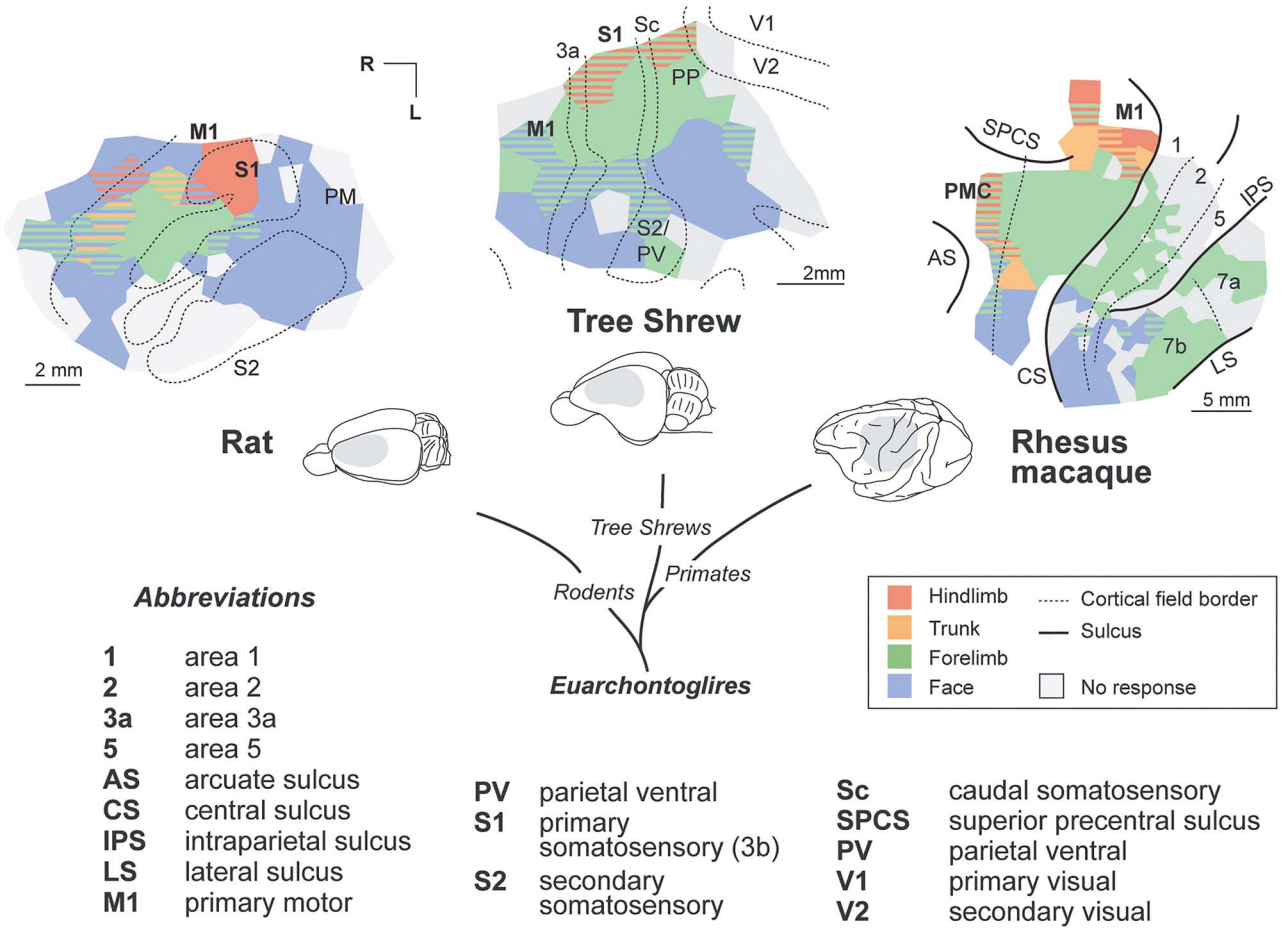

Figure 9. Comparative studies of motor cortex from our laboratory show how species within the evolutionary clade *Euarchontoglires* differ in movements elicited by LT-ICMS. Simplified body-part maps are shown for individual cases in rat (current study), tree shrew (Baldwin et al. 2017a), and macaque (Baldwin et al. 2018). Movements can be evoked from both M1 and S1 in each species, with enlarged movement representations of the face in rats and the forelimb in primates. Primates also have several premotor and posterior parietal areas not observed in other species from which movements can be evoked. Data sources: rat (present study), tree shrew (Baldwin et al. 2017a), and macaque (Baldwin et al. 2018).

stimulation of S1 (area 3b) still elicits movements (Baldwin et al. 2017b), suggesting a distinct role for S1 in motor control, separate from frontal motor regions (Matyas et al. 2010).

The Evolution of Motor Cortex in Mammals

The current findings require that we revisit theories of motor cortex evolution in mammals that utilized data from rats and other rodents to substantiate the major claims of these theories. To appreciate the relevance of this, we must step back to the middle of the last century when Lende explored the sensory and motor cortex of marsupials (Lende 1963a, 1963b). Using evoked potential recordings and cortical stimulation to explore sensory and motor cortex in the Virginia opossum and the wallaby, he found that marsupials have a complete overlap of the primary somatosensory area and the primary motor area, which he called a "sensorimotor amalgam" (Lende 1963a, 1963b, 1969). His proposition was that marsupial sensorimotor cortex represents a primitive state of organization in which areas S1 and M1, as described in placental mammals, are completely overlapping, and that the evolution of this cortex in eutherian mammals is marked by a progressive separation of these fields, ultimately into two complete and separate sensory (S1) and motor (M1) representations (Fig. 8A) (Lende 1969; see Karlen and Krubitzer 2007 for review). An intermediate stage of this progressive separation, the partial overlap of S1 and M1, was thought to exist in rats (Fig. 8B), and the complete separation of sensory and motor cortex was thought to have emerged in primates. As noted above, recent ICMS studies in a variety of primates and nonprimate mammals require that we revisit the basic assumptions of this theory, since the data that gave rise to it have been supplemented by more complete datasets in a number of mammals. For example, preliminary ICMS research on the short-tailed opossum *Monodelphis domestica* indicate that a distinct motor field, rostral to the "amalgam," exists in marsupials (Halley et al. 2019).

The current results suggest that similar to other eutherians, movements in the rat can be elicited from stimulation of most of histologically defined S1 (Fig. 8E) and not simply the small region of forelimb and hindlimb overlap proposed under the "amalgam" hypothesis (Fig. 8B). Specifically, the involvement of S1 in generating whisker movements is difficult to reconcile with a partial overlap of mirror-reversed motor and sensory representations, given that the whisker regions in S1 and M1 are not adjacent (i.e., the motor functions in S1 cannot be due to an overlap with M1). An interpretation better supported by recent

evidence is that rodents do not occupy an intermediate position between marsupials and primates (e.g., Frost et al. 2000) but instead have an S1 with motor functions, like primates and other eutherian mammals (Fig. 8D). Rather than S1 and M1 becoming parcellated (Ebbesson 1980) from an ancestral sensorimotor "amalgam," (Lende 1969), independent motor areas may have been added, and S1 has retained its role in motor functions in all extant mammals (Beck et al. 1996).

Thus, a common feature of organization in eutherian mammals is the presence of an S1 and M1, each of which has different patterns of connectivity and plays a different functional role in motor control (Fig. 9). However, important differences exist between species related to specializations in body morphology and the unique behaviors species exhibit (e.g., forelimbs used in grasping versus flying). In primates, the representation of the hand in cortical areas in frontal and parietal cortex is enormous, movements of individual digits can be evoked, and movements resembling precision grips in which D1 is opposed to one or more other digits can also be evoked. Likewise, the number of cortical fields involved in motor control is greatly increased in some lineages, such as primates (Halley and Krubitzer 2019), and include premotor, supplementary motor, areas 1 and 2, and regions of posterior parietal cortex. The evolution of motor control therefore likely involves both the expansion of existing representations within cortical areas, the addition of new motor areas, and the anatomical and functional specialization of each area associated with the sensorimotor demands of different body morphologies, environments, and behaviors.

Supplementary Material

Supplementary material can be found at *Cerebral Cortex* online.

Funding

McDonnell Foundation (220020516 to L.K.); National Eye Institute (5T32EY015387-15 to A.C.H.).

Notes

Thanks to Cynthia Weller, Ryan Manning, Heather Dodson, and Carlos Pineda for experimental assistance, and Karen Zito for providing animals used in this study. Histological sections were scanned in Ted Jones Microscopy Laboratory at the Center for Neuroscience at UC Davis. *Conflict of Interest*: None declared.

References

Auffret M, Ravano VL, Rossi GMC, Hankov N, Petersen MFA, Petersen CCH. 2018. Optogenetic stimulation of cortex to map evoked whisker movements in awake head-restrained mice. *Neuroscience*. 368:199–213.

Baldwin MKL, Cooke DF, Krubitzer L. 2017a. Intracortical microstimulation maps of motor, somatosensory, and posterior parietal cortex in tree shrews (*Tupaia belangeri*) reveal complex movement representations. *Cereb Cortex*. 27:1439–1456.

Baldwin MKL, Halley AC, Krubitzer L. 2017b. The functional organization of movement maps in new world titi monkeys. *Soc Neurosci Abstr*. 48:316.06.

Baldwin MKL, Cooke DF, Goldring AB, Krubitzer L. 2018. Representations of fine digit movements in posterior and anterior parietal cortex revealed using long-train intracortical microstimulation in macaque monkeys. *Cereb Cortex*. 28: 4244–4263.

Beck PD, Pospichal MW, Kaas JH. 1996. Topography, architecture, and connections of somatosensory cortex in opossums: evidence for five somatosensory areas. *J Comp Neurol*. 366:109–133.

Bonazzi L, Viaro R, Lodi E, Canto R, Bonifazzi C, Franchi G. 2013. Complex movement topography and extrinsic space representation in the rat forelimb motor cortex as defined by long-duration intracortical microstimulation. *J Neurosci*. 33:2097–2107.

Brecht M, Krauss A, Muhammad S, Sinai-Esfahani L, Bellanca S, Margrie TW. 2004. Organization of rat vibrissa motor cortex and adjacent areas according to cytoarchitectonics, microstimulation, and intracellular stimulation of identified cells. *J Comp Neurol*. 479:360–373.

Brown AR, Teskey GC. 2014. Motor cortex is functionally organized as a set of spatially distinct representations for complex movements. *J Neurosci*. 34:13574–13585.

Burish MJ, Stepniewska I, Kaas JH. 2008. Microstimulation and architectonics of frontoparietal cortex in common marmosets (Callithrix jacchus). *J Comp Neurol*. 507:1151–1168.

Clemens AM, Delgado YF, Mehlman ML, Mishra P, Brecht M. 2018. Multisensory and motor representations in rat oral somatosensory cortex. *Sci Rep*. 8:13556.

Cooke DF, Taylor CS, Moore T, Graziano MS. 2003. Complex movements evoked by microstimulation of the ventral intraparietal area. *Proc Natl Acad Sci USA*. 100:6163–6168.

Cooke DF, Padberg J, Zahner T, Krubitzer L. 2012. The functional organization and cortical connections of motor cortex in squirrels. *Cereb Cortex*. 22:1959–1978.

Cooke DF, Stepniewska I, Miller DJ, Kaas JH, Krubitzer L. 2015. Reversible deactivation of motor cortex reveals functional connectivity with posterior parietal cortex in prosimian galago (Otolemur garnetti). *J Neurosci*. 35:14406–14422.

Dawson DR, Killackey HP. 1987. The organization and mutability of the forepaw and hindpaw representations in the somatosensory cortex of the neonatal rat. *J Comp Neurol*. 256:246–256.

Deffeyes JE, Touvykine B, Quessy S, Dancause N. 2015. Interactions between rostral and caudal cortical motor areas in the rat. *J Neurophysiol*. 113:3893–3904.

Disbrow E, Roberts T, Krubitzer L. 2000. Somatotopic organization of cortical fields in the lateral sulcus of Homo sapiens: evidence for SII and PV. *J Comp Neurol*. 418:1–21.

Donoghue JP, Wise SP. 1982. The motor cortex of the rat: cytoarchitecture and microstimulation mapping. *J Comp Neurol*. 212:76–88.

Ebbesson SOE. 1980. The parcellation theory and its relation to interspecific variability in brain organization, evolutionary and ontogenetic development, and neuronal plasticity. *Cell Tissue Res*. 213:179–212.

Frost SB, Garrett MW, Plautz EJ, Masterton RB, Nudo RJ. 2000. Somatosensory and motor representations in cerebral cortex of a primitive mammals (Monodelphis domestica): a window into the early evolution of sensorimotor cortex. *J Comp Neurol*. 421:29–51.

Gharbawie OA, Stepniewska I, Qi H, Kaas JH. 2011. Multiple parietal-frontal pathways mediate grasping in macaque monkeys. *J Neurosci*. 31:11660–11677.

Gioanni Y, Lamarche M. 1985. A reappraisal of rat motor cortex organization by intracortical microstimulation. *Brain Res*. 344:49–61.

Graziano MS, Taylor CS, Moore T, Cooke DF. 2002. The cortical control of movement revisited. *Neuron*. 36:349–362.

Hall RD, Lindholm EP. 1974. Organization of motor and somatosensory neocortex in the albino rat. *Brain Res*. 66:23–38.

Halley AC, Krubitzer L. 2019. Not all cortical expansions are the same: the coevolution of the neocortex and the dorsal thalamus in mammals. *Curr Opin Neurobiol*. 56:78–86.

Halley AC, Baldwin MKL, Englund M, Sanchez A, Krubitzer L. 2019. Intracortical microstimulation of sensorimotor cortex in short-tailed opossum (*Monodelphis domestica*): new insights into the evolution of motor cortex in mammals. *Soc Neurosci Abstr*. 49:494.08.

Halley AC, Yartsev MM, Krubitzer L. 2018. The organization of motor cortex in the Egyptian fruit bat (*Rousettus aegyptiacus*): specializations of the tongue representation associated with echolocation. *Soc Neurosci Abstr*. 48:24.

Hamadjida A, Dea M, Deffeyes J, Quessy S, Dancause N. 2016. Parallel cortical networks formed by modular organization of primary motor cortex outputs. *Curr Biol*. 26:1737–1743.

Kaas JK. 1982. The segregation of function in the nervous system: why do the sensory systems have so many subdivisions? Contribution to. *Sens Phys*. 7:88–117.

Kaas JH. 1983. What, if anything, is SI? Organization of first somatosensory area of cortex. *Physiol Rev*. 63:206–231.

Karadimas SK, Satkunendrarajah K, Laliberte AM, Ringuette D, Weisspapir I, Li L, Gosgnach S, Fehlings MG. 2020. Sensory cortical control of movement. *Nat Neurosci*. 23:75–84.

Karl JM, Sacrey L-AR, McDonald RJ, Whishaw IQ. 2008. Intact intracortical microstimulation (ICMS) representations of rostral and caudal forelimb areas in rats with quinolinic acid lesions of the medial or lateral caudate-putamen in an animal model of Huntington's disease. *Brain Res Bull*. 77: 42–48.

Karlen SJ, Krubitzer L. 2007. The functional and anatomical organization of marsupial neocortex: evidence for parallel evolution in mammals. *Prog Neurobiol*. 82:122–141.

Krubitzer L, Campi KL, Cooke DF. 2011. All rodents are not the same: a modern synthesis of cortical organization. *Brain Behav Evol*. 78:51–93.

Lende RA. 1963a. Sensory representation in the cerebral cortex of the opossum (Didelphis virginiana). *J Comp Neurol*. 121:395–403.

Lende RA. 1963b. Motor representation in the cerebral cortex of the opossum (Didelphis virginiana). *J Comp Neurol*. 121:405–415.

Lende RA. 1969. A comparative approach to the neocortex: localization in monotremes, marsupials and insectivores. *Ann N Y Acad Sci*. 167:262–276.

Li X-G, Florence SL, Kaas JH. 1990. Areal distributions of cortical neurons projecting to different levels of the caudal brain stem and spinal cord in rats. *Sens Motor Res*. 7:315–335.

Liu L-Y, Guo D-S, Xin X-Y, Fang J. 2008. Observation of a system of linear loops formed by re-growing hairs on rat skin. *Anat Rec*. 291:858–868.

Matyas F, Sreenivasan V, Marbach F, Wacongne C, Barsy B, Bateo C, Aronoff R, Petersen CCH. 2010. Motor control by sensory cortex. *Science*. 330:1240–1243.

Mayer A, Baldwin MKL, Cooke DF, Lima BR, Padberg J, Lewenfus G, Franca JG, Krubitzer L. 2019. The multiple representations of complex digit movements in primary motor cortex form the building blocks for complex grip types in capuchin monkeys. *J Neurosci*. 39:6684–6695.

Mohammed H, Jain N. 2016. Ipsilateral cortical inputs to the rostral and caudal motor area in rats. *J Comp Neurol*. 524:3104–3123.

Neafsey EJ, Sievert C. 1982. A second forelimb motor area exists in the rat frontal cortex. *Brain Res*. 232:151–156.

Neafsey EJ, Bold EL, Haas G, Hurley-Gius KM, Quirk G, Sievert CF, Terreberry RR. 1986. The organization of the rat motor cortex: a microstimulation mapping study. *Brain Res*. 396:77–96.

Ramanathan D, Conner JM, Tuszynski MH. 2006. A form of motor cortical plasticity that correlates with recovery of function after brain injury. *Proc Natl Acad Sci USA*. 103:11370–11375.

Rathelot J-A, Dum RP, Strick PL. 2017. Posterior parietal cortex contains a command apparatus for hand movements. *Proc Natl Acad Sci USA*. 114:4255–4260.

Remple MS, Henry EC, Catania KC. 2003. Organization of somatosensory cortex in the laboratory rat (Rattus norvegicus): evidence for two lateral areas joined at the representation of the teeth. *J Comp Neurol*. 467:105–118.

Rouiller EM, Moret V, Liang F. 1993. Comparison of the connectional properties of the two forelimb areas of the rat sensorimotor cortex: support for the presence of a premotor and supplementary motor area. *Somatosens Mot Res*. 10:269–289.

Sapienza S, Talbi B, Jacquemin J, Albe-Fessard D. 1981. Relationship between input and output of cells in motor and somatosensory cortices of the chronic awake rat. *Exp Brain Res*. 43:47–56.

Seelke AM, Padberg JJ, Disbrow E, Purnell SM, Recanzone G, Krubitzer, L. 2012. Topographic maps within Brodmann's area 5 of macaque monkeys. *Cereb Cortex*. 22:1834–1850.

Sreenivasan V, Karmaker K, Filippo MR, Petersen CCH. 2015. Parallel pathways from motor and somatosensory cortex for controlling whisker movement in mice. *Eur J Neurosci*. 41:354–367.

Stepniewska I, Fang P-C, Kaas JH. 2005. Microstimulation reveals specialized subregions for different complex movements in posterior parietal cortex of prosimian galagos. *Proc Natl Acad Sci USA*. 102:4878–4883.

Strick PL. 2002. Stimulating research on motor cortex. *Nat Neurosci*. 5:714–715.

Tandon S, Kambi N, Jain N. 2008. Overlapping representations of the neck and whiskers in the rat motor cortex revealed by mapping at different anesthetic depths. *Eur J Neurosci*. 27:228–237.

Tennant KA, Adkins DL, Donlan NA, Asay AL, Thomas N, Kleim JA, Jones TA. 2010. The organization of the forelimb representation of the C57BL/6 mouse motor cortex as defined by intracortical microstimulation and cytoarchitecture. *Cereb Cortex*. 21:865–876.

Welker WI, Benjamin RM, Miles RC, Woolsey CN. 1957. Motor effects of stimulation of cerebral cortex of squirrel monkey (Saimiri sciureus). *J Neurophysiol*. 20:347–364.

Woolsey CN. 1958. Organization of somatic sensory and motor areas of the cerebral cortex. In: Harlow HF, Woolsey CN, editors. *The biological and biochemical basis of behavior*. Madison: University of Wisconsin Press, pp. 63–81.

Woolsey CN, Erickson TC, Gilson WE. 1979. Localizaton in somatic sensory and motor areas of human cerebral cortex as determined by direct recording of evoked potentials and electrical stimulation. *J Neurosurg*. 51:476–506.

Wu CW, Bichot NP, Kaas JH. 2000. Converging evidence from microstimulation, architecture, and connections for multiple motor arears in the frontal and cingulate cortex of prosimian primates. *J Comp Neurol*. 423:140–177.